Evidence for Structural Changes in Carboxyl-Terminal Peptides of Transducin α-Subunit upon Binding a Soluble Mimic of Light-Activated Rhodopsin†

D. M. Brabazon,*,‡ N. G. Abdulaev,§ J. P. Marino,§ and K. D. Ridge*,§

Department of Chemistry, Loyola College in Maryland, Baltimore, Maryland 21210, and Center for Advanced Research in Biotechnology, National Institute of Standards and Technology and University of Maryland Biotechnology Institute, Rockville, Maryland 20850

Received September 23, 2002; Revised Manuscript Received November 5, 2002

ABSTRACT: Although a high-resolution crystal structure for the ground state of rhodopsin is now available, portions of the cytoplasmic surface are not well resolved, and the structural basis for the interaction of the cytoplasmic loops with the retinal G-protein transducin (G_t) is still unknown. Previous efforts aimed at the design, construction, and functional characterization of soluble mimics for the light-activated state of rhodopsin have shown that grafting defined segments from the cytoplasmic region of bovine opsin onto a surface loop in a mutant form of thioredoxin (HPTRX) is sufficient to confer partial G_t activating potential [Abdulaev et al. (2000) *J. Biol. Chem. 275*, 39354−39363]. To assess whether these designed mimics could provide a structural insight into the interaction between light-activated rhodopsin and G_t, the ability of an HPTRX fusion protein comprised of the second (CD) and third (EF) cytoplasmic loops (HPTRX/CDEF) to bind G_t α-subunit ($G_{t\alpha}$) peptides was examined using nuclear magnetic resonance (NMR) spectroscopy. Transfer NOESY (TrNOESY) experiments show that an 11 amino acid peptide corresponding to the carboxyl terminus of $G_{t\alpha}$ (GtP), as well as a "high-affinity" peptide analogue, HAP1, binds to HPTRX/CDEF in the fast-exchange regime and undergoes similar, subtle structural changes at the extreme carboxyl terminus. Observed TrNOEs suggest that both peptides when bound to HPTRX/CDEF adopt a reverse turn that is consistent with the C-cap structure that has been previously reported for the interaction of GtP with the light-activated signaling state, metarhodopsin II (MII). In contrast, TrNOESY spectra provide no evidence for structuring of the amino terminus of either GtP or HAP1 when bound to HPTRX/CDEF, nor do the spectra show any measurable changes in the CD and EF loop resonances of HPTRX/CDEF, which are conformationally dynamic and significantly exchange broadened. Taken together, the NMR observations indicate that HPTRX/CDEF, previously identified as a functional mimic of MII, is also an approximate structural mimic for this light-activated state of rhodopsin.

G-protein-coupled receptors (GPCRs)[1] are a diverse group of sensory and nonsensory seven transmembrane (TM) helix receptors that require ligand-dependent activation to initiate G-protein-mediated intracellular signaling cascades. Rhodopsin, the rod cell photoreceptor involved in dim light vision, represents one of the best studied GPCRs in terms of structure and function (*1*, *2*). Light triggers the cis → trans isomerization of the retinal chromophore buried within the seven TM helical bundle. This change in retinal configuration is thought to initiate structural changes in the TM helices, resulting in the formation of the light-activated signaling state, metarhodopsin II (MII). At MII, small, yet functionally significant changes occur in the solvent-exposed cytoplasmic loops that lead to the formation of binding and activation sites for several signaling proteins, including the retinal G-protein transducin (G_t) (*3*−*13*).

Rhodopsin is the only GPCR for which high-resolution structural information is currently available. The ground (dark) state crystal structure of bovine rhodopsin (*14*) confirmed the presence of the seven TM helices and highlighted several new structural features including a "plug" comprised of multiple intradomain contacts on the extracellular surface and an eighth amphipathic helix extending from the seventh TM that forms a part of the cytoplasmic

† This work was supported by Grant CC5250 from Research Corp. to D.M.B., NIH Grants EY11112 and EY13286, and a Karl Kirchgessner Foundation award to K.D.R. J.P.M. is supported by NIH Grant GM59107. NMR instrumentation was supported in part by the W. M. Keck Foundation. This is paper 5 in the series Folding and Assembly in Rhodopsin. Reference *58* is paper 4 in the series.

* Corresponding authors. D.M.B.: tel, 410-617-2236; fax, 410-617-2803; e-mail, dbrabazon@loyola.edu. K.D.R.: tel, 301-738-6218; fax, 301-738-6255; e-mail, ridge@carb.nist.gov.

‡ Loyola College in Maryland.

§ National Institute of Standards and Technology and University of Maryland Biotechnology Institute.

[1] Abbreviations: GPCRs, G-protein-coupled receptors; G-protein, guanine nucleotide-binding protein; TM, transmembrane; MII, metarhodopsin II; ROS, rod outer segment; G_t, G-protein transducin; $G_{t\alpha}$, α-subunit of G_t; GtP, carboxyl-terminal peptide of $G_{t\alpha}$; HAP1, high-affinity analogue of the carboxyl-terminal peptide of $G_{t\alpha}$; HPTRX, His-patch thioredoxin; EDTA, ethylenediaminetetraacetic acid; DTT, dithiothreitol; NTA, nitrilotriacetic acid; NMR, nuclear magnetic resonance spectroscopy; NOE, nuclear Overhauser effect; TrNOESY, transferred nuclear Overhauser enhancement spectroscopy; ROESY, rotating frame Overhauser enhancement spectroscopy; TOCSY, total correlation spectroscopy; HSQC, heteronuclear single-quantum correlation spectroscopy; 1D, one dimensional; 2D, two dimensional; τ_c, correlation time. Single- and three-letter abbreviations are used for amino acids.

10.1021/bi0268899 CCC: $25.00
Published on Web 12/21/2002

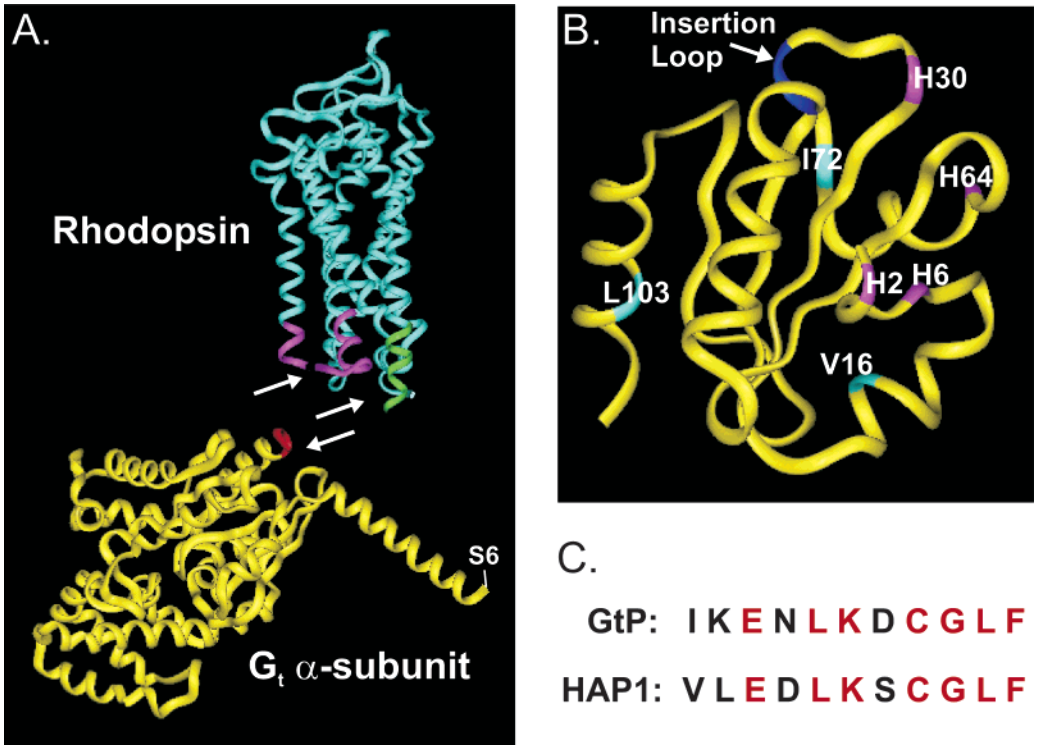

FIGURE 1: (A) Model for the interaction between the CD and EF loops of rhodopsin with the carboxyl terminus of $G_{t\alpha}$. Sequences of interest are highlighted: residues 132−142 and 148−154 representing the CD loop of rhodopsin (magenta), residues 243−252 representing the EF loop in rhodopsin (green), and residues 340−343 of the carboxyl terminus of $G_{t\alpha}$ (red). Arrows are pointing to regions where additional residues in the CD and EF loops and the carboxyl terminus of $G_{t\alpha}$ could not be fit to the electron density due to high *B*-factors. Ser-6, representing the amino terminus of $G_{t\alpha}$, is labeled. The images were generated using InsightII (Accelrys, Inc.) and PDB files 1F88 for the ground-state crystal structure of rhodopsin and 1GOT for the crystal structure of $G_{t\alpha\beta\gamma}$. (B) Three-dimensional structural model for HPTRX based on the structure of thioredoxin (PDB file 2TRX). The histidine residues at positions 2, 6, 30, and 62, which form a three-dimensional His-patch, are labeled and highlighted (magenta). The site of opsin CD and/or EF loop insertion(s) between Pro-34 and Cys-35 is indicated (blue) and labeled with an arrow. The three residues with resolved methyl resonances used to confirm fusion protein structural integrity are labeled and highlighted (turquoise). (C) Amino acid sequences of the GtP and HAP1 peptides. Conserved residues between the peptides are shown in red.

surface. A recent refinement of the structure has provided a more detailed view of the TM region and the retinal binding pocket (*15*). However, current structural models for rhodopsin (Figure 1A) are incomplete as they lack resolvable electron density in portions of the cytoplasmic loop regions connecting some of the TM helices. Specifically, Gln-236 through Ser-240 is absent in molecule A and Lys-141 through Phe-148, as well as Val-227 through Thr-243, is missing from molecule B (*14*). These sequences correspond to portions of the second (CD) and third (EF) cytoplasmic loops, the major interaction sites for G_t (*16*−*32*), rhodopsin kinase (*33*−*38*), and arrestin (*39*−*43*). Further, the ground-state structure provides few clues into the mechanism of receptor activation and the ensuing structural changes that are required for function.

Binding of heterotrimeric G-proteins to activated GPCRs requires the presence of both the G-protein α- and $\beta\gamma$-subunits. Three regions on $G_{t\alpha}$ are known to be important for receptor interactions: the amino-terminal 23 residues, an internal sequence from amino acids 311−329, and the carboxyl-terminal 11 amino acids (*44*). Some important insights into the mechanism of G-protein-mediated signal transduction have been provided through high-resolution structures of G_α (*45*−*50*) and $G_{\beta\gamma}$ (*51*) subunits, as well as $G_{\alpha\beta\gamma}$ heterotrimeric complexes (*52*, *53*). In most of the crystal structures, the residues at the extreme amino and carboxyl termini of G_α are disordered and/or not visible (Figure 1A). This is consistent with several NMR studies (*54*−*57*) of 11 amino acid carboxyl-terminal peptides derived from $G_{t\alpha}$, $G_{t\alpha}$-(340−350), which indicate that these peptides are largely unstructured in solution. In contrast, the NMR studies also revealed that these $G_{t\alpha}$ peptides undergo significant structural changes upon binding to the light-activated state of rhodopsin in rod outer segment (ROS) membranes (*54*−*57*). These further findings suggest a direct interaction between the carboxyl-terminal residues of $G_{t\alpha}$ and rhodopsin.

Previously, we reported work on the design, expression, and functional characterization of soluble mimics for the light-activated state of rhodopsin (*58*). These mimics were prepared by grafting defined segments from the cytoplasmic surface of bovine opsin, either singly or in combination, onto a mutant thioredoxin (HPTRX) scaffold (Figure 1B; ref *59*). Biochemical studies showed that anchoring specific portions of the cytoplasmic loops connecting helices C and D and E and F onto HPTRX was sufficient to allow these segments to adopt a conformation that confers G_t activating potential, albeit to a significantly lower extent than observed for light-activated rhodopsin (*58*). This reduced level of G_t activation is apparently due to the fact that the interaction of HPTRX/CDEF with G_t is not catalytic; i.e., while a single light-activated rhodopsin can activate numerous G_t molecules, each HPTRX/CDEF appears only capable of binding and/or activating a single G_t. These findings raise the possibility that this or similarly designed rhodopsin mimics may be

useful for obtaining not only approximate structural information about the light-activated conformation of the CD and EF loops but also the binding sites for interacting proteins (or fragments of these proteins). This is especially advantageous since a high-resolution structure of a ligand-activated GPCR in complex with its cognate G-protein may not be immediately forthcoming.

The goal of this study was therefore to investigate whether synthetic peptides corresponding to the carboxyl-terminal region of $G_{t\alpha}$ are able to bind to HPTRX/CDEF and, if so, to potentially identify structural changes in both molecules that might arise from this interaction. For this purpose, the interaction between HPTRX/CDEF and two 11 amino acid peptides (Figure 1C) that correspond to the native carboxyl-terminal sequence of $G_{t\alpha}$ (GtP) and a "high-affinity" analogue (HAP1) was examined by nuclear magnetic resonance (NMR) spectroscopy. Importantly, these peptides have been extensively characterized for their ability to bind and stabilize the MII conformation of light-activated ROS rhodopsin (*26*, *44*, *60*−*63*). The present results show that both GtP and HAP1 bind to HPTRX/CDEF and undergo similar, subtle structural changes at the extreme carboxyl terminus in the bound state. Observed transferred nuclear Overhauser effects (TrNOEs) suggest that both peptides form a reverse turn that is consistent with an α_L-type C-cap in the bound state, as has been previously reported for the interaction of $G_{t\alpha}$ peptides with MII. In contrast, TrNOESY spectra provide no evidence for significant structuring of the amino-terminal amino acids of either GtP or HAP1 when bound to HPTRX/CDEF, nor do the spectra show any detectable changes in NMR resonances associated with HPTRX/CDEF. The ability of HPTRX/CDEF to interact with these peptides and confer conformational changes in a manner analogous to light-activated ROS rhodopsin suggests that this designed protein is an approximate structural, as well as functional, mimic of the light-activated signaling state. In addition, the observation of significant conformational exchange broadening of the CD and EF loop amino acid resonances in HPTRX/CDEF indicates that these loops are highly dynamic and implies that HPTRX/CDEF samples multiple conformational states in rapid equilibrium, among which is a "MII-like" state.

MATERIALS AND METHODS[2]

Peptide and Protein Sample Preparation. The acetylated carboxyl-terminal $G_{t\alpha}$ peptides (Figure 1C), GtP (amino acids 340−350) and HAP1 (an analogue of GtP) (*60*−*63*), were from Biosynthesis Incorporated (Lewisville, TX). The lyophilized peptides were resuspended in buffer A (25 mM Tris-HCl, 100 mM NaCl, 1 mM EDTA, 0.1 mM DTT) and adjusted to pH ~7.5 on ice and a final concentration of 4 mM. HPTRX, HPTRX/EF, and HPTRX/CDEF were expressed and purified on Ni^{2+}-NTA−agarose as previously described (*58*). HPTRX, HPTRX/EF, and HPTRX/CDEF were also expressed in minimal media containing ^{15}N-labeled ammonium chloride (CIL, Andover, MA) as the sole nitrogen source for heteronuclear NMR spectral studies. NMR samples contained the respective protein (0.50 mM) in 25 mM d_{11}-Tris-HCl, pH 7.0, 100 mM NaCl, 1 mM EDTA, 0.1 mM DTT, and 10% ^2H_2O. NMR binding experiments were taken using a final peptide concentration of 2 mM.

NMR Spectroscopy. All experiments were collected on a Bruker DMX 500 spectrometer at 278 K**,** unless otherwise indicated, using an HCN triple resonance probe with triple axis actively shielded pulsed field gradients. One-dimensional (1D) proton and ^{15}N-filtered proton spectra were collected with spectral widths of 6009 Hz and 2048 complex points and 64 and 128 scans, respectively. H_2O suppression was achieved using a water-flip back, Watergate pulse sequence. Two-dimensional (2D) TOCSY (total correlation spectroscopy), NOESY (nuclear Overhauser effect spectroscopy), and ROESY (rotating frame Overhauser enhancement spectroscopy) spectra were collected with 256 × 2048 complex points and 32 scans per t_1 point. For the TOCSY experiment, a DIPSI-2 mixing sequence of 36 ms, flanked by two 2 ms trim pulses, a 0.5 s preacquisition delay, and 1.0 s of H_2O presaturation, was used. NOESY spectra were collected with T_{NOE} mixing periods ranging from 200 to 400 ms and ROESY spectra with a T_{ROE} of 200 ms. The data were processed using NMRPipe (*64*) and analyzed with SPARKY (*65*) on a LINUX/PC workstation.

RESULTS

NMR Analysis of HPTRX, HPTRX/EF and HPTRX/CDEF. Uniformly ^{15}N-labeled HPTRX, HPTRX/EF, and HPTRX/CDEF were first investigated using 1D proton and ^{15}N-filtered NMR experiments to assay for the solubility and folded state of these engineered proteins in the micromolar to millimolar concentration range. Figure 2 shows the amide and upfield aliphatic regions of a 1D ^{15}N-decoupled proton spectra for HPTRX, HPTRX/EF, and HPTRX/CDEF collected at 303 K. The spectra clearly show that insertion of the EF loop and the CD and EF loops into HPTRX results in significant broadening of amide proton signals associated with HPTRX residues, with observed broadening for HPTRX/CDEF being considerably larger than for HPTRX/EF. In addition, new amide proton signals associated with the inserted loop amino acid sequences are observed that cluster in a narrow chemical shift range centered around 8.0 ppm. In all of these spectra, the observations of signature HPTRX methyl group resonances between 0.2 and −0.8 ppm (assignments are indicated in Figure 2 and corresponding amino acids highlighted in Figure 1B) serve as a confirmation of the fact that loop insertion does not result in the misfolding or unfolding of HPTRX. This result was expected since the protein purification scheme requires proper folding of HPTRX (i.e., formation of a three-dimensional His-patch; Figure 1B) that allows for high-affinity binding and separation using a Ni^{2+}-NTA column.

Two-dimensional ^{15}N heteronuclear single-quantum coherence (HSQC) and ^{15}N-edited NOESY spectra (data not shown) were collected for HPTRX, HPTRX/EF, and HPTRX/CDEF to resolve and assign the amide resonances associated with the inserted CD and EF loops. However, the significant broadening of amide resonances associated with HPTRX along with the poor dispersion of the inserted loop amide resonances made it difficult to fully assign the

[2] Certain commercial materials, instruments, and equipment are identified in this manuscript in order to specify the experimental procedure as completely as possible. In no case does such identification imply a recommendation by the National Institute of Standards and Technology nor does it imply that the materials, instruments, or equipment identified are necessarily the best available for the purpose.

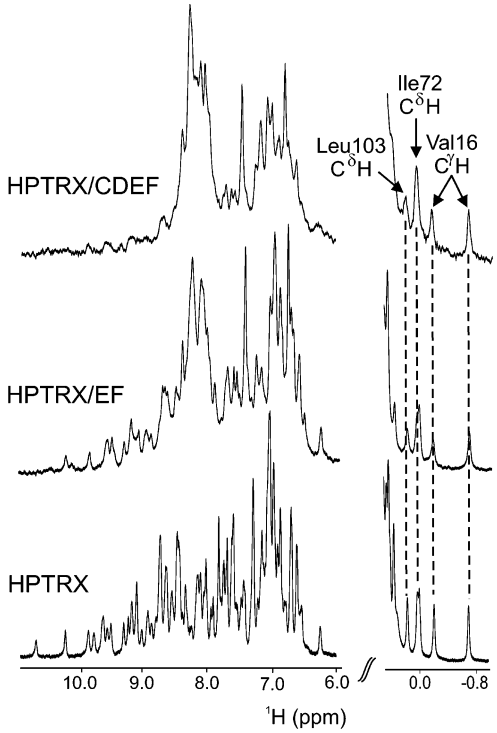

FIGURE 2: One-dimensional (1D) NMR spectral comparisons of the amide and upfield methyl regions of the three ^{15}N-labeled proteins: HPTRX, HPTRX/EF, and HPTRX/CDEF. The EF and CD/EF loop insertions significantly broaden the amide proton resonances of HPTRX in the HPTRX/EF and HPTRX/CDEF spectra. In these same samples, the chemical shift and intensity of signature HPTRX methyl proton resonances are also clearly observed to remain unperturbed, indicating proper folding of all the proteins. Assignments for these HPTRX methyl proton resonances are labeled.

HPTRX/EF and HPTRX/CDEF spectra. The NMR data suggest that the loops in HPTRX/EF and HPTRX/CDEF, which have been *restrained* by insertion into HPTRX in order to mimic the light-activated form of the native receptor, are not characterized by one well-ordered structure but are most likely highly dynamic. The dynamic character of the loops can be inferred from the relative sharpness of the amide signals associated with the inserted loop residues with respect to the amide signals of HPTRX, which could result from faster motions of the loop residues that are uncorrelated to the overall correlation time (τ_c) of HPTRX/CDEF. Such motions could also account for the observed broadening of HPTRX signals by propagating intermediate time-scale dynamic fluctuations through the HPTRX backbone sequence surrounding the loop insertion point. The lack of resolvable electron density for portions of these two cytoplasmic loops in the ground-state crystal structure of rhodopsin (*14*) is consistent with these observations.

Interaction of $G_{t\alpha}$ Carboxyl-Terminal Peptides with HPTRX/CDEF As Monitored by NMR Spectroscopy. In systems where exchange rates between free and bound forms of a ligand are comparable to or faster than the rate at which cross-relaxation in the bound state takes place, standard NMR methods can be applied to excess free ligand to study the conformation of the bound ligand. Moreover, since cross-relaxation processes in the slowly tumbling complex normally dominate, NOESY spectra collected on such rapidly exchanging systems detect interproton distances that almost exclusively represent the bound ligand conformation. The interaction of $G_{t\alpha}$ peptides with rhodopsin in ROS membranes occurs in the fast-exchange regime, and the conformations of bound peptides have been characterized in previous studies using such transferred NOESY (TrNOESY) methods (*54*−*57*). These studies have demonstrated that the $G_{t\alpha}$ peptides adopt specific conformations upon interaction with light-activated ROS rhodopsin.

To determine whether analogous structuring occurs when $G_{t\alpha}$ peptides are bound to HPTRX/CDEF, NMR methods have been utilized to probe any potential interaction. Only HPTRX/CDEF has been pursued in this study since our previous work indicated a requirement for insertion of both the CD and EF loops into the HPTRX scaffold to confer G_t activating potential (*58*). ^{15}N-Labeled HPTRX/CDEF was first titrated with either GtP or HAP1 and monitored using 1D ^{15}N/^{14}N-filtered/edited proton NMR spectroscopy. ^{15}N/^{14}N-filtered/edited 1D proton spectra were collected to allow selective observation of amide resonances from either HPTRX/CDEF (^{15}N-selected) or the peptides (^{14}N-edited) during the course of the titration. The titration was carried out to a final peptide concentration of 2 mM and a stoichiometric ratio of 4:1 (peptide:HPTRX/CDEF). Overall, the line widths of the proton resonances of both the GtP and HAP1 peptides showed only slight broadening as a result of the titration. In addition, the chemical shifts of the peptide proton resonances from GtP and HAP1, as well as HPTRX/CDEF, did not exhibit any significant changes during the course of the titration. These results indicated that any potential binding interaction is characterized by a fast-exchange regime. Thus, unlike light-activated ROS rhodopsin, HPTRX/CDEF does not appear to discriminate between the "native" (GtP) and high-affinity (HAP1) forms of the $G_{t\alpha}$ peptide. In addition, since the affinity of both peptides for HPTRX/CDEF is weak, TrNOESY methods could be used to characterize these interactions.

Since the chemical shifts of proton resonances from both GtP and HAP1 did not change significantly during the course of the titration, both peptides could be assigned (Table 1) in the free state from a combination of 2D NOESY, ROESY, and TOCSY experiments. The assignments for both peptides are quite similar and in good agreement with those made previously using GtP and the peptide analogue S2 (*55*−*57*) and indicate that these peptides are quite structurally similar to each other as would be expected on the basis of their close sequence homology (Figure 1C). Since macromolecules with molecular masses of around 1 kDa tumble at a τ_c close to the zero crossing of the NOE function, a ROESY experiment was applied to both the GtP and HAP1 peptides to see if any additional NOEs could be observed that may have been too weak to be detected in the NOESY experiment. The ROESY experiment generated the same pattern of NOEs as observed in the NOESY experiment, without any additional correlations. Thus, the NOESY and ROESY experiments confirm that the GtP and HAP1 peptides display no stable long-range structure in solution.

Structural Changes in GtP upon Binding to HPTRX/CDEF. By comparison of the 2D NOESY experiments of GtP alone (data not shown) and in the presence of HPTRX/CDEF (Figure 3), a few additional NOE cross-peaks have been identified and the intensity of some NOE cross-peaks in the spectrum of the peptide−HPTRX/CDEF mixture have changed, indicating that GtP indeed binds to HPTRX/CDEF

Table 1: Proton Resonance Assignments (in ppm) for GtP and HAP1[a]

residue	NH	αH	βH	γH	δH	others
Ile-340	8.10	3.88	1.81			δCH_3 0.69, γCH_3 97, γCH_2 1.26
(Val)	(8.05)	(3.63)	(1.78)			(γCH_3 0.69)
Lys-341	8.36	4.12	1.61, 1.56	1.23	1.48	
(Leu)	(8.26)	(3.78)	(1.40)	(1.32)		(δCH_3 0.68, 0.62)
Glu-342	8.36	4.01	1.80, 1.73	2.04		
	(8.25)	(4.11)	(1.76, 1.67)	(2.00)		
Asn-343	8.45	4.48	2.65, 2.54			
(Asp)	(8.22)	(4.33)	(2.48, 2.35)			
Leu-344	8.20	4.12	1.46	1.40		δCH_3 0.67, 0.71
	(8.11)	(4.19)	(1.41)	(1.34)		(δCH_3 0.67, 0.60)
Lys-345	8.16	4.06	1.60	1.45	1.20	
	(8.18)	(4.06)	(1.58)	(1.40)	(1.19)	
Asp-346	8.25	4.40	2.56, 2.46			
(Ser)	(8.18)	(4.19)	(3.63)			
Cys-347	8.19	4.29	2.76			
	(8.33)	(4.19)	(2.99, 2.76)			
Gly-348	8.40	3.72				
	(8.33)	(3.65)				
Leu-349	7.83	4.09	1.30	1.23		δCH_3 0.66
	(7.82)	(4.05)	(1.26)	(1.19)		(δCH_3 0.63, 0.56)
Phe-350	7.57	4.24	2.97, 2.74			δ(2,4) 6.98, ϵ(3,5) 7.09
	(7.51)	(4.17)	(2.91, 2.69)			(δ(2,4) 6.93, ϵ(3,5) 7.04)

[a] HAP1 assignments are shown in parentheses.

in the fast-exchange regime. It is important to note that because HPTRX/CDEF is considered to be a constitutive mimic of light-activated rhodopsin, NMR measurements could be readily acquired over long time periods without the technical problems associated with MII decay. The additional NOE cross-peaks that are observed in the presence of HPTRX/CDEF for the most part involve amino acids in the extreme carboxyl terminus of the peptide. In particular, the NOESY spectra of GtP in the presence of HPTRX/CDEF displays two new sets of NOEs between the F350 Hδ and Hϵ protons and the Hβ protons and Hα of F350, which are not observed in the free state of the peptide. This indicates that the F350 side chain is ordered upon binding to HPTRX/CDEF in two bound conformational states that are in slow exchange. In addition, long-range NOE correlations are observed between both sets of F350 Hδ and Hϵ protons and the Hδ protons of L344 (boxed in Figure 3A), although the set marked with an asterisk in Figure 3 clearly appears to display weaker NOEs relative to the other. Interestingly, these NOEs are similar to those observed in previous studies (*55*−*57*) and are consistent with the formation of an α_L-type C-cap in the bound state of GtP.

Sequential $^1H^N-^1H^N$ NOE connectivities between the carboxyl-terminal amino acid residues F350, L349, and G348 are also observed in the GtP-bound state (Figure 3B). Of these $^1H^N-^1H^N$ NOE cross-peaks, only F350NH−L349NH is found in the NOESY spectrum of free GtP, confirming the results of previous studies (*54*, *56*) that indicated that $G_{t\alpha}$ peptides do not exhibit any significant structure when free in solution. These NOEs further suggest a structuring of the extreme carboxyl terminus of the peptide upon interaction with HPTRX/CDEF, which would be expected upon formation of the C-cap motif. In contrast, the absence of sequential $^1H^N-^1H^N$ NOE connectivities between the amino-terminal amino acids, as well as a lack of additional NOEs indicative of α-helix geometry in the TrNOESY

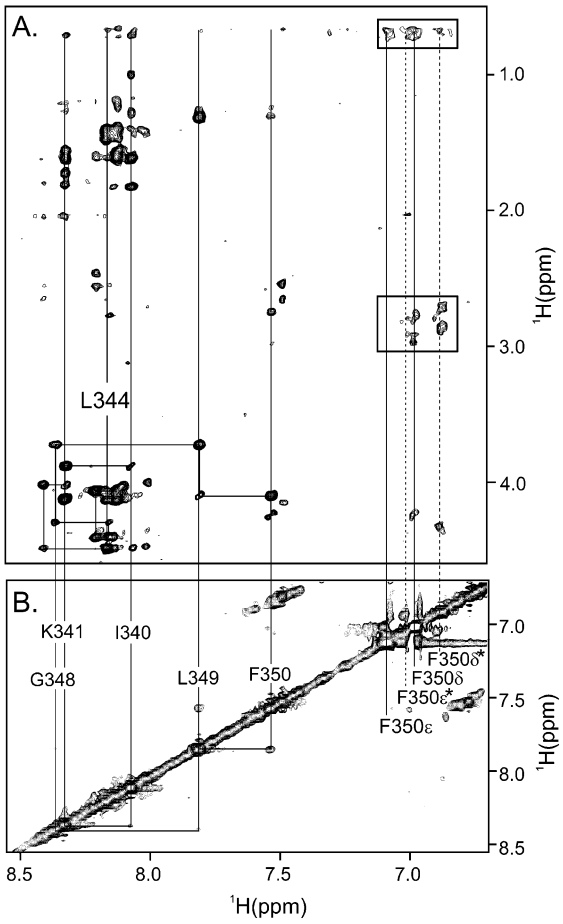

FIGURE 3: Two-dimensional ^{14}N-edited TrNOESY spectrum at 278 K of the mixture of GtP peptide with HPTRX/CDEF in a ratio of 4:1 (peptide:HPTRX/CDEF). (A) Expansion of the amide to aliphatic region of the TrNOESY spectra with the sequential H^N-H^α correlations indicated by lines and amide proton resonances between which additional TrNOEs are observed in the bound state indicated by vertical lines. Additional long-range TrNOEs involving the F350 side chain Hδ and Hϵ protons that are observed in the bound state are boxed. (B) Expansion of the amide to amide region of the TrNOESY spectra with the $^1H^N_i-^1H^N_{i+1}$ carboxyl-terminal TrNOEs observed between residues F350, L349, and G348 connected by lines and labeled with assignments.

spectra of GtP in the presence of HPTRX/CDEF, suggests that the amino-terminal amino acids of GtP do not adopt any detectable secondary structure upon binding to HPTRX/CDEF. In comparison, an almost complete set of $^1H^N-^1H^N$ NOE cross-peaks, as well as other long-range NOEs, has been observed for GtP when bound to light-activated ROS rhodopsin (*55*), indicating that the amino-terminal amino acids assumed an α-helical conformation.

Structural Changes in HAP1 upon Binding to HPTRX/CDEF. In the NOESY spectra of free HAP1 (data not shown), weak $^1H^N_i-^1H^N_{i+1}$ cross-peaks are observed between amino acids at the carboxyl terminus of the peptide and between the Hβ and Hδ protons of F350, indicating that this high-affinity peptide has some inherent structure independent of binding to HPTRX/CDEF which is not observed in the GtP peptide. The NOESY spectrum of the free HAP1 peptide, however, shows no evidence for long-range NOEs and, in particular, no NOEs specifically involving the F350 side chain protons.

Comparison of the 2D NOESY experiments of HAP1 alone and in the presence of HPTRX/CDEF (Figure 4) again

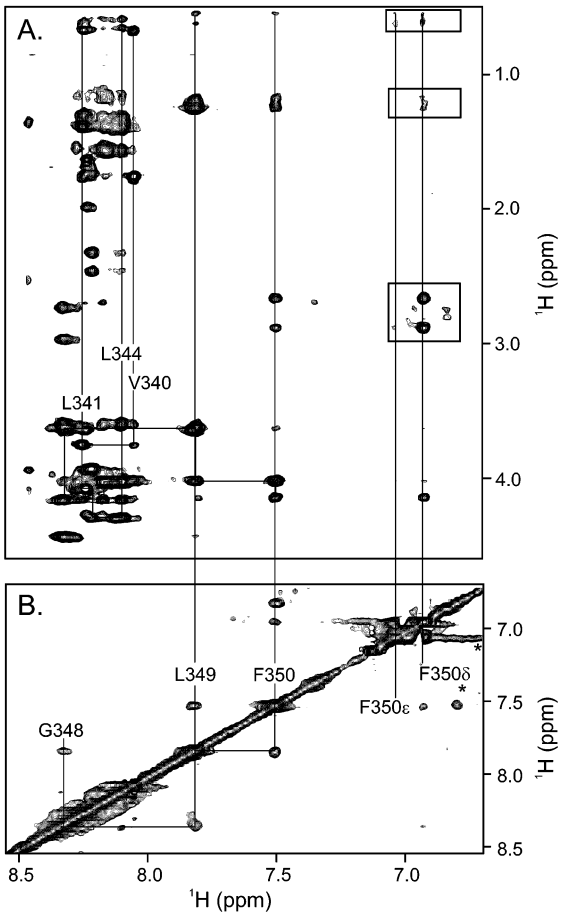

FIGURE 4: Two-dimensional ^{14}N-edited TrNOESY spectrum at 278 K of the mixture of HAP1 peptide with HPTRX/CDEF in a ratio of 4:1 (peptide:HPTRX/CDEF). (A) Expansion of the amide to aliphatic region of the TrNOESY spectra with the sequential H^N-H^α correlations indicated by lines and amide proton resonances between which additional TrNOEs are observed in the bound state indicated by vertical lines. Additional long-range TrNOEs involving the F350 side chain Hδ and Hϵ protons that are observed in the bound state are boxed. (B) Expansion of the amide to amide region of the TrNOESY spectra with the $^1H^N_i-^1H^N_{i+1}$ carboxyl-terminal TrNOEs observed between residues F350, L349, and G348 connected by lines and labeled with assignments.

allows a few additional NOE cross-peaks to be identified, and the intensity of some NOE cross-peaks in the spectrum of the peptide−HPTRX/CDEF mixture have changed, indicating that HAP1 binds to HPTRX/CDEF in the fast-exchange regime. Upon binding to HPTRX/CDEF, HAP1 appears to structure in a manner that is quite similar to that observed for GtP. Unlike GtP, however, only a single set of resonances is observed for the F350 side chain of HAP1. Nonetheless, long-range NOE correlations are again observed for HAP1 between the F350 Hδ and Hϵ protons and the Hδ protons of L341 and L349 (boxed in Figure 4A). These NOEs are strikingly similar to those observed for GtP bound to HPTRX/CDEF (Figure 3), as well as previous studies with $G_{t\alpha}$ peptides and ROS membranes (*55*−*57*).

Sequential $^1H^N-^1H^N$ NOE connectivities between the carboxyl-terminal amino acid residues F350, L349, and G348 are observed to increase significantly in the HAP1-bound state (Figure 4B). These NOEs again suggest a stabilization of the structure of the extreme carboxyl terminus of the peptide upon interaction with HPTRX/CDEF, which would be expected with the formation of a C-cap. As compared to the GtP peptide, the $^1H^N-^1H^N$ NOEs observed for HAP1 appear to be relatively stronger, indicating a more structurally stable state for this peptide both when free and in complex with HPTRX/CDEF. In contrast to previous work (*54*−*57*), sequential $^1H^N-^1H^N$ NOE connectivities between the amino-terminal amino acids, as well as a lack of additional NOEs indicative of α-helix geometry, again indicate that this region of HAP1 does not adopt any detectable secondary structure upon binding to HPTRX/CDEF.

In addition to the observation of new NOEs in the TrNOE spectra of bound GtP and HAP1, differences in NOE peak volumes and line-widths of cross-peaks between the bound and free spectra also indicate that these peptides interact with HPTRX/CDEF. For both peptides, the most significant changes in NOE peak volumes are localized to amino acids at the extreme carboxyl-terminal end of the peptide. However, the number of additional medium- and long-range TrNOEs observed for the bound states of both peptides is insufficient to allow the determination of high-resolution structural models at this time.

Specificity of the GtP and HAP1 Peptide Interaction with HPTRX/CDEF. To verify that the observed changes in the GtP and HAP1 peptide NOESY spectra upon interaction with HPTRX/CDEF were the result of specific contacts made between the inserted CD and EF loops and the GtP and HAP1 peptides, TrNOESY experiments were collected under identical conditions using HPTRX. Importantly, the TrNOEs observed in these experiments show no evidence for binding of either peptide to HPTRX, demonstrating that the presence of the CD and/or EF loops on HPTRX/CDEF is necessary for the interaction (data not shown).

Structural Changes in HPTRX/CDEF upon GtP and HAP1 Peptide Binding. Analysis of the HPTRX/CDEF proton and nitrogen resonances upon addition of either GtP or HAP1, correlated in ^{15}N−HSQC and ^{15}N-filtered NOESY experiments, showed no significant changes in either chemical shift, line-width, or NOE cross-peak pattern (data not shown). This negative result may be a consequence of the fact that peptide binding does not confer any significant structural organization to the CD and EF loops or more likely that the significant conformational exchange broadening observed for the loop amino acids precludes reliable detection of any likely subtle structural changes.

DISCUSSION

As a first step toward understanding the molecular details of how the intracellular signaling cascade is initiated for GPCRs, a number of studies have sought to identify specific contacts between $G_{t\alpha}$ and the cytoplasmic surface of light-activated rhodopsin. Previous efforts along these lines have focused primarily on mutagenesis studies of rhodopsin and $G_{t\alpha}$ as well as varying peptide sequences corresponding to the carboxyl terminus of $G_{t\alpha}$. For rhodopsin, it has been shown that defined segments and specific amino acids in the second (CD) and third (EF) cytoplasmic loops, as well as in the fourth loop (helix 8) formed from the end of the seventh TM to the Cys-322/Cys-323 palmitoylation sites, are important for the binding and/or activation of G_t (*19*−*31*). Mutagenesis studies on $G_{t\alpha}$ have also highlighted specific amino acids that participate in rhodopsin binding from those which are required for intrinsic activity (*30*, *31*, *66*, *67*), while

numerous synthetic peptides corresponding to the carboxyl-terminal 11 amino acids of $G_{t\alpha}$, $G_{t\alpha}$-(340−350), have been shown to mimic the conformational effect of G_t by stabilizing the MII photointermediate and/or competitively blocking MII−G_t interactions (*26*, *44*, *60*−*63*). More recently, cross-linking studies have been used to identify sites of contact between the EF loop of light-activated rhodopsin and the amino- and carboxyl-terminal regions of $G_{t\alpha}$ (*68*, *69*). Collectively, these advances have provided valuable clues about the sites of interaction on both light-activated rhodopsin and G_t. However, the molecular details governing this interaction, which ultimately triggers the visual transduction process, remain largely unknown. Thus, the goal of this study was to investigate whether synthetic peptides corresponding to the carboxyl-terminal region of $G_{t\alpha}$ and a soluble mimic for the light-activated form of rhodopsin (HPTRX/CDEF) could serve as a useful model system for elucidating how specific structural changes are coupled to signaling by the native receptor.

The 1D proton spectrum for HPTRX/CDEF shows that insertion of the CD and EF loops into HPTRX results in a significant broadening of amide proton signals associated with HPTRX residues (Figure 2). Further, new amide proton signals associated with the inserted loops are observed that cluster in a narrow chemical shift range around 8.0 ppm. These results suggest that HPTRX/CDEF has an increased structural flexibility compared to HPTRX, as well as HPTRX/EF. Additional HPTRX/opsin fragment fusion proteins have also shown significant conformational flexibility. For example, HPTRX/ABCDEF (*58*), which also contains an inserted sequence corresponding to the AB (first) cytoplasmic loop in addition to the CD and EF loops, exhibited exchange-broadened NMR spectra that could not be interpreted in any detail (D. M. Brabazon, N. G. Abdulaev, J. P. Marino, and K. D. Ridge, unpublished observations). Thus, the dynamic nature of the inserted CD and EF loops, rather than unfolded or misfolded protein, appears responsible for the clustering and broadening of amide resonances. As indicated earlier, these results were not too surprising since the high crystallographic *B*-factors for this region of the rhodopsin crystal structure (*14*) prevented the electron density to be completely fit, suggesting a highly dynamic character for these loops. Furthermore, they are also consistent with solution ^{19}F NMR studies showing a highly dynamic nature for rhodopsin's cytoplasmic surface in both the dark- and light-activated states (*70*).

Both peptide interactions with HPTRX/CDEF are weak with rapid off-rates that may result from the fact that this fusion protein represents a mimic of the light-activated conformation of rhodopsin where such rapid binding kinetics would be favored. Although the relative affinities of each peptide for HPTRX/CDEF are not known since they cannot be determined from the NMR data, it appears that HPTRX/CDEF does not discriminate to a significant degree between the native (GtP) and high-affinity (HAP1) forms of the $G_{t\alpha}$ peptide. This is in stark contrast to light-activated ROS rhodopsin, where affinities for the GtP and HAP1 peptides differ by 2 orders of magnitude (*63*). Thus, while HPTRX/CDEF is capable of binding both native and high-affinity $G_{t\alpha}$ carboxyl-terminal peptides, it appears to lack certain rhodopsin elements that confer this distinctive property. Nevertheless, since both peptides bind in the fast-exchange regime, TrNOESY methods could be used in this study to characterize the conformation of the bound state of the peptide. Such TrNOESY methods have previously been exploited (*55*) to characterize the bound state of GtP with light-activated ROS rhodopsin and indicated a significant structuring of this peptide upon binding that involved helical formation of the amino terminus and a C-cap at the carboxyl terminus. A recent study (*57*) has similarly utilized the measurement of additional transferred dipolar couplings to determine a refined structure for a bound analogue of the GtP peptide, S2, as well as the orientation of the peptide relative to the ROS membrane surface.

Here, NMR structural analysis of the HPTRX/CDEF bound form of GtP and HAP1 reveals that although both peptides undergo apparently similar structural changes, neither is fully converted to the structured form observed in the presence of intact, light-activated ROS rhodopsin. Our results suggest that both the GtP and HAP1 peptides adopt a structure at the carboxyl terminus (Figures 3 and 4) that is analogous to the capping of the carboxyl terminus of GtP and S2 observed in the presence of light-activated ROS rhodopsin (*55*−*57*) and, similarly, is distinct from that reported by Dratz et al. (*54*) using another $G_{t\alpha}$ peptide. However, in contrast to these same studies where α-helix formation was observed for the amino terminus, no evidence for a similar structuring of the amino terminus of either GtP or HAP1 when bound to HPTRX/CDEF was found. Thus, HPTRX/CDEF may not contain all of the receptor elements that are necessary for inducing the full complement of changes observed previously (*55*−*57*). In this context, it should be mentioned that work from Karnik and colleagues (*26*) has shown that residues Tyr-136 through Val-139 of the CD loop and residues Glu-247 through Thr-251 of the EF loop form the binding site on light-activated rhodopsin for GtP. Further, additional mutagenesis studies (*19*) have shown that the Glu-134/Arg-135 charge pair in the CD loop is important for G_t binding/activation. Since HPTRX/CDEF contains all of these essential elements, it is likely that other factors, including some that may not necessarily be related to the inclusion of a particular amino acid(s), might contribute to the observed differences in the structural changes imparted to the $G_{t\alpha}$ peptides upon binding to HPTRX/CDEF. These factors could include imperfections in mimicry of the MII structural organization of the CD and EF loops in HPTRX/CDEF, the absence of a lipid bilayer, or, less likely, deleterious interactions between the CD and/or EF loops and HPTRX. At this point, we cannot firmly exclude the possibility of a requirement for other opsin cytoplasmic surface sequences, such as those found in the fourth loop (helix 8), that have been shown to be involved in G_t activation and $G_{t\alpha}$ carboxyl-terminal peptide binding (*28*, *29*). While it is clear that HPTRX/CDEF does not possess all of the functional properties of MII in terms of the G_t interaction, it is anticipated that further efforts focused on the design and characterization of additional mimics, which so far remain a largely empirical endeavor, will allow us to discern between these possibilities.

Figure 5 shows a summary representation of the TrNOE evidence for the reverse turn structuring of the GtP and HAP1 peptides upon binding to HPTRX/CDEF mapped onto the structure of the α_L-type C-cap seen in the bound GtP peptide from the study of Kisselev et al. (*55*). Amino acid residues

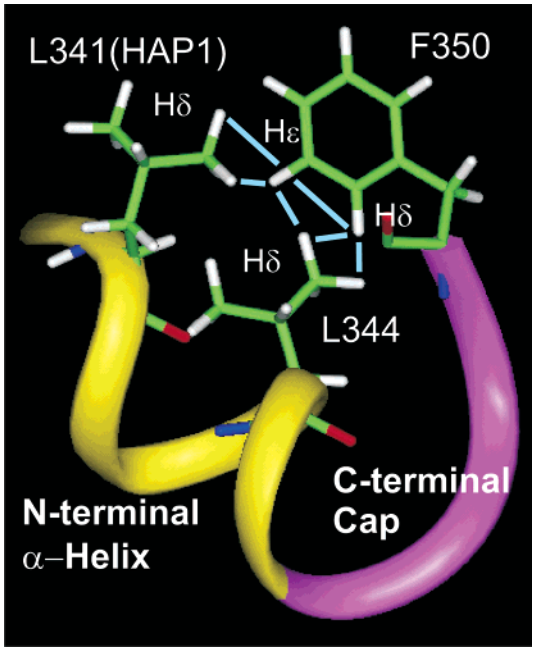

FIGURE 5: Summary representation of the common TrNOEs observed for the GtP and HAP1 peptides upon binding to HPTRX/CDEF mapped onto the structure of the light-activated ROS rhodopsin-bound GtP peptide from the NMR study of Kisselev et al. (*55*). The image was generated using InsightII (Accelrys, Inc.) and 1 of the 20 structures from the ensemble deposited collectively as PDB file 1AQG. Amino acid residues in the carboxyl-terminal C-cap region of the GtP structure, for which corresponding $^1H^N_i$–$^1H^N_{i+1}$ NOEs are observed in the HPTRX/CDEF bound spectra of both peptides, are shown as a magenta ribbon, and amino acid residues in the amino terminus, for which NOEs indicative of α-helical geometry are not observed in the HPTRX/CDEF bound spectra of both peptides, are shown as a yellow ribbon. Long-range TrNOEs between the side chain protons of F350 and L344 observed for GtP and between F350 and L341 observed for HAP1 observed in the present study are mapped onto the GtP structure using solid blue lines.

in the carboxyl-terminal region, for which $^1H^N_i$–$^1H^N_{i+1}$ are observed in the HPTRX/CDEF bound spectra of both peptides (Figures 3 and 4), are shown as a magenta ribbon, and amino acid residues in the amino terminus, for which α-helical NOEs are not observed in the HPTRX/CDEF bound spectra of both peptides, are shown as a yellow ribbon. Specific long-range NOE contacts are also indicated between the side chain protons of F350 and L344 in GtP and F350 and L341 in HAP1. It is surprising that these long-range NOEs are observed despite the lack of an apparent structuring of the amino terminus, as evidenced by the lack of backbone-associated NOEs in either HPTRX/CDEF bound peptide. One possible dynamic explanation for these observations may be intermediate conformational exchange for the peptide backbone in the bound state which is uncoupled from a more rapid conformational exchange of the side chains. In such a model, averaged long-range NOEs would be observed, while backbone NOEs might be too broad to be detected. Alternatively, the data may indicate that the interaction with HPTRX/CDEF is sufficient for inducing only a clustering of hydrophobic side chains, or formation of a so-called hydrophobic patch (*63*), while not completely stabilizing the backbone geometry of the C-cap reverse turn to the same extent as light-activated ROS rhodopsin.

Amino acid changes in the GtP peptide sequence have been shown to affect binding to wild-type rhodopsin. Substitutions in the carboxyl-terminal portion of the peptide (*26*, *60*−*63*) or in the corresponding region of $G_{t\alpha}$ (*66*, *67*) dramatically influence the interaction with MII. Since the extreme carboxyl terminus of the peptide adopts a defined structure upon interaction with light-activated rhodopsin (*54*−*57*), proper function would appear to be coupled to this folding transition. For both GtP and HAP1, some structural changes are also observed upon binding to HPTRX/CDEF (Figures 3 and 4). The ability of HPTRX/CDEF to activate G_t only at significantly lower levels than observed for light-activated ROS rhodopsin (*58*), however, may be related to the observation of only partial structuring of the $G_{t\alpha}$ peptides. Previously, it was suggested that the reduced level of G_t activation is due to the fact that HPTRX/CDEF does not catalytically interact with G_t. Taken together, this raises the possibility that the noncatalytic behavior of HPTRX/CDEF may be related to its inability to propagate helical structure in the carboxyl-terminal region of $G_{t\alpha}$. As indicated above, however, this may also be due to design imperfections in HPTRX/CDEF that result in a CD/EF loop binding surface topology that does not exactly match that present on light-activated ROS rhodopsin.

A more detailed comparison of the TrNOESY results obtained here for the GtP and HAP1 peptides reveals some potential clues into the structural and dynamical differences between these two peptides that lead to the significant differences in their binding affinity for light-activated ROS rhodopsin. The NOESY/ROESY experiments contain cross-peaks that indicate free HAP1 has some structure toward the carboxyl terminus of the peptide sequence (Figure 4B). In contrast, the observation of a single weak cross-peak (F350NH−L349NH) visible in similar NMR experiments of free GtP (Figure 3B) confirmed the results of previous studies (*54*, *56*, *57*), indicating that GtP and its analogues do not exhibit any significant structure when free in solution. The observation of difference in apparent structure and stability between the two peptides might account for the difference in binding affinity for light-activated ROS rhodopsin (*63*). In addition, the observation of a significantly higher quality TrNOESY spectrum for the bound HAP1 peptide when compared to GtP (i.e., more observed medium- and long-range NOEs in the HAP1-bound state versus the GtP-bound state) and the indication in the GtP-bound state TrNOESY spectrum that the carboxyl-terminal F350 residue experiences conformational exchange also hint that a predisposition of the HAP1 peptide to form a single "active" conformation may be the basis for its observed high-affinity. Nevertheless, the difference in the degree of preorganization and the overall relative structural stability of the carboxyl terminus of HAP1 does not appear to allow HPTRX/CDEF to discriminate between these two peptides in a significant way.

CONCLUSION

This study represents the first example of an engineered soluble protein that appears to function through a structural mechanism that is analogous to what has been observed for an intact, activated GPCR (light-activated rhodopsin). The dynamic nature of the interaction between the $G_{t\alpha}$ peptides and HPTRX/CDEF indicates that formation of a reverse turn in the carboxyl-terminal region of these peptides is not accompanied by a stable helical transition in the amino-terminal region. Thus, while the mechanism of $G_{t\alpha}$ peptide

structuring by HPTRX/CDEF is sufficiently close to that of MII, at least in regard to the formation of the hydrophobic patch on the $G_{t\alpha}$ peptides, other crucial elements of the MII interacting surface responsible for stable helical organization of the 340−346 amino acid stretch are apparently lacking. This may have implications for understanding the molecular basis of the noncatalytic nature of the interaction between HPTRX/CDEF and G_t. Although structural changes were evident in both $G_{t\alpha}$ peptides as a result of binding to HPTRX/CDEF, any corresponding conformational changes in the CD and EF loops that may complete this *molecular handshake* were not apparent. The conformational exchange observed for the CD and EF loops in HPTRX/CDEF, combined with the lack of resolvable electron density in the corresponding portions of the rhodopsin crystal structure (*14*) and the findings from recent solution ^{19}F NMR studies (*70*), strongly suggests that the cytoplasmic surface of rhodopsin is highly dynamic. Since the methods described here provide access to models for the solution state(s) of GPCRs and their interactions with G-proteins, the design and expression of soluble mimics for other GPCRs could provide distinct advantages for studying the structure and function of these critical components of various signal transduction pathways.

ACKNOWLEDGMENT

We thank T. Ngo (CARB), L. Massey, and A. Sweigart (Loyola College in Maryland) for technical assistance with protein expression and purification.

REFERENCES

1. Okada, T., Ernst, O. P., Palczewski, K., and Hofmann, K. P. (2001) *Trends Biochem. Sci. 26*, 318−325.
2. Sakmar, T. P. (2001) *Curr. Opin. Cell Biol. 14*, 189−195.
3. Kühn, H., Mommertz, O., and Hargrave, P. A. (1982) *Biochim. Biophys. Acta 679*, 95−100.
4. Pellicone, C., Nullans, G., Cook, N., and Virmaux, N. (1985) *Biochem. Biophys. Res. Commun. 127*, 816−821.
5. Farahbakhsh, Z. T., Hideg, K., and Hubbell, W. L. (1993) *Science 262*, 1416−1419.
6. Resek, J. F., Farahbakhsh, Z. T., Khorana, H. G., and Hubbell, W. L. (1993) *Biochemistry 32*, 12025−12031.
7. Farahbakhsh, Z. T., Ridge, K. D., Khorana, H. G., and Hubbell, W. L. (1995) *Biochemistry 34*, 8812−8819.
8. Altenbach, C., Yang, K., Farrens, D. L., Khorana, H. G., and Hubbell, W. L. (1996) *Biochemistry 35*, 12470−12478.
9. Abdulaev, N. G., and Ridge, K. D. (1998) *Proc. Natl. Acad. Sci. U.S.A. 95*, 12854−12859.
10. Altenbach, C., Cai, K., Khorana, H. G., and Hubbell, W. L. (1999) *Biochemistry 38*, 7931−7937.
11. Altenbach, C., Klein-Seetharaman, J., Hwa, J., Khorana, H. G., and Hubbell, W. L. (1999) *Biochemistry 38*, 7945−7949.
12. Altenbach, C., Cai, K., Klein-Seetharaman, J., Khorana, H. G., and Hubbell, W. L. (2001) *Biochemistry 40*, 15483−15492.
13. Altenbach, C., Klein-Seetharaman, J., Cai, K., Khorana, H. G., and Hubbell, W. L. (2001) *Biochemistry 40*, 15493−15500.
14. Palczewski, K., Kumasaka, T., Hori, T., Behnke, C. A., Motoshima, H., Fox, B. A., Le Trong, I., Teller, D. C., Okada, T., Stenkamp, R. E., Yamamoto, M., and Miyano, M. (2000) *Science 289*, 739−745.
15. Okada, T., Fujiyoshi, Y., Silow, M., Navarro, J., Landau, E. M., and Schichida, Y. (2002) *Proc. Natl. Acad. Sci. U.S.A. 99*, 5982−5987.
16. Takemoto, D. J., Morrison, D., Davis, L. C., and Takemoto, L. J. (1986) *Biochem. J. 235*, 309−312.
17. Weiss, E. R., Kelleher, D. J., and Johnson, G. L. (1988) *J. Biol. Chem. 263*, 2119−2122.
18. König, B., Arendt, A., McDowell, J. H., Kahlert, M., Hargrave, P. A., and Hofmann, K. P. (1989) *Proc. Natl. Acad. Sci. U.S.A. 86*, 6878−6882.
19. Franke, R. R., König, B., Sakmar, T. P., Khorana, H. G., and Hofmann, K. P. (1990) *Science 250*, 123−125.
20. Franke, R. R., Sakmar, T. P., Graham, R. M., and Khorana, H. G. (1992) *J. Biol. Chem. 267*, 14767−14774.
21. Min, K. C., Zvyaga, T. A., Cypess, A. M., and Sakmar, T. P. (1993) *J. Biol. Chem. 268*, 9400−9404.
22. Shi, W., Osawa, S., Dickerson, C. D., and Weiss, E. R. (1995) *J. Biol. Chem. 270*, 2112−2119.
23. Ridge, K. D., Zhang, C., and Khorana, H. G. (1995) *Biochemistry 34*, 8804−8811.
24. Yang, K., Farrens, D. L., Hubbell, W. L., and Khorana, H. G. (1996) *Biochemistry 35*, 12464−12469.
25. Acharya, S., and Karnik, S. S. (1996) *J. Biol. Chem. 271*, 25406−25411.
26. Acharya, S., Saad, Y., and Karnik, S. S. (1997) *J. Biol. Chem. 272*, 6519−6524.
27. Cai, K, Klein-Seetharaman, J., Farrens, D., Zhang, C., Altenbach, C., Hubbell, W. L., and Khorana, H. G. (1999) *Biochemistry 38*, 7925−7930.
28. Marin, E. P., Krishna, A. G., Zvyaga, T. A., Isele, J., Siebert, F., and Sakmar, T. P. (2000) *J. Biol. Chem. 275*, 1930−1936.
29. Ernst, O. P., Meyer, C. K., Marin, E. P., Henklein, P., Fu, Y., Sakmar, T. P., and Hofmann, K. P. (2000) *J. Biol. Chem. 275*, 1937−1943.
30. Yamashita, T., Terakita, A., and Shichida, Y. (2000) *J. Biol. Chem. 275*, 34272−34279.
31. Terakita, A., Yamashita, T., Nimbari, N., Kojima, D., and Shichida, Y. (2002) *J. Biol. Chem. 277*, 40−46.
32. Hamm, H. E. (2001) *Proc. Natl. Acad. Sci. U.S.A. 98*, 1715−1720.
33. Palczewski, K., McDowell, J. H., and Hargrave, P. A. (1988) *Biochemistry 27*, 2306−2313.
34. Kelleher, D. J., and Johnson, G. L. (1990) *J. Biol. Chem. 265*, 2632−2639.
35. Palczewski, K., Buczylko, J., Kaplan, M. W., Polans, A, S., and Crabb, J. W. (1991) *J. Biol. Chem. 266*, 12949−12955.
36. Brown, N. G., Fowles, C., Sharma, R., and Akhtar, M. (1992) *Eur. J. Biochem. 208*, 659−667.
37. Rim, J., Faurobert, E., Hurley, J. B., and Oprian, D. D. (1997) *Biochemistry 36*, 7064−7070.
38. Thurmond, R. L., Creuzenet, C., Reeves, P. J., and Khorana, H. G. (1997) *Proc. Natl. Acad. Sci. U.S.A. 94*, 1715−1720.
39. Krupnick, J. G., Gurevich, V. V., Schepers, T., Hamm, H. E., and Benovic, J. L. (1994) *J. Biol. Chem. 269*, 3226−3232.
40. Puig, J., Arendt, A., Tomson, F. L., Abdulaeva, G., Miller, R., Hargrave, P. A., and McDowell, J. H. (1995) *FEBS Lett. 362*, 185−189.
41. Wu, G. Y., Krupnick, J. G., Benovic, J. L., and Lanier, S. M. (1997) *J. Biol. Chem. 272*, 17836−17842.
42. Shi, W., Sports, C. D., Raman, D., Shirakawa, S., Osawa, S., and Weiss, E. R. (1998) *Biochemistry 37*, 4869−4874.
43. Raman, D., Osawa, S., and Weiss, E. R. (1999) *Biochemistry 38*, 5117−5123.
44. Hamm, H. E., Deretic, D., Arendt, A., Hargrave, P. A., Koenig, B., and Hoffman, K. P. (1988) *Science 241*, 832−835.
45. Coleman, D. E., Berghuis, A. M., Lee, E., Linder, M. E., Gilman, A. G., and Sprang, S. R. (1994) *Science 269*, 1405−1412.
46. Lambright, D. G., Noel, J. P., Hamm, H. E., and Sigler, P. B. (1994) *Nature 369*, 621−628.
47. Mixon, M. B., Lee, E., Coleman, D. E., Berghuis, A. M., Gilman, A. G., and Sprang, S. R. (1995) *Science 270*, 954−960.
48. Noel, J. P., Hamm, H. E., and Sigler, P. B. (1993) *Nature 366*, 654−663.
49. Sondek, J., Lambright, D. G., Noel, J. P., Hamm, H. E., and Sigler, P. B. (1994) *Nature 372*, 276−279.
50. Sunahara, R. K., Tesmer, J. J., Gilman, A. G., and Sprang, S. R. (1997) *Science 278*, 1943−1947.
51. Sondek, J., Bohm, A., Lambright, D. G., Hamm, H. E., and Sigler, P. B. (1996) *Nature 379*, 369−374.
52. Lambright, D. G., Sondek, J., Bohm, A., Skiba, N. P., Hamm, H. E., and Sigler, P. B. (1996) *Nature 379*, 311−319.
53. Wall, M. A., Coleman, D. E., Lee, E., Iniguez-Lluhi, J. A., Posner, B. A., Gilman, A. G., and Sprang, S. R. (1995) *Cell 83*, 1047−1058.

54. Dratz, E. A., Furstenau, J. E., Lambert, C. G., Thireault, D. L., Rarick, H., Schepers, T., Pakhlevaniants, S., and Hamm, H. E. (1993) *Nature 363*, 276−281; Dratz, E. A, Furstenau, J. E., Lambert, C. G., Thireault, D. L., Rarick, H., Schepers, T., Pakhlevaniants, S., and Hamm, H. E. (1997) *Nature 390*, 424 (correction).
55. Kisselev, O. G., Kao, J., Ponder, J. W., Fann, Y. C., Gautam, N., and Marshall, G. R. (1998) *Proc. Natl. Acad. Sci. U.S.A. 95*, 4270−4275.
56. Koenig, B. W., Mitchell, D. C., Konig, S., Grzesiek, S., Litman, B. J., and Bax, A. (2000) *J. Biomol. NMR 16*, 121−125.
57. Koenig, B. W., Kontaxis, G., Mitchell, D. C., Louis, J. M., Litman, B. J., and Bax, A. (2002) *J. Mol. Biol. 322*, 441−461.
58. Abdulaev, N. G., Ngo, T., Chen, R., Lu, Z., and Ridge, K. D. (2000) *J. Biol. Chem. 275*, 39354−39363.
59. Lu, Z., DiBlasio-Smith, E. A., Grant, K. A., Warne, N. W., LaVallie, E. R., Collins-Racie, L. A., Follettie, M. T., Williamson, M. J., and McCoy, J. M. (1996) *J. Biol. Chem. 271*, 5059−5065.
60. Rasenick, M. M., Watanabe, M., Lazarevic, M. B., Hatta, S., and Hamm, H. E. (1994) *J. Biol. Chem. 269*, 21519−21528.
61. Martin, E. L., Rens-Domiano, S., Schatz, P. J., and Hamm, H. E. (1996) *J. Biol. Chem. 271*, 361−366.
62. Aris, L., Gilchrist, A., Rens-Domiano, S., Meyer, C., Schatz, P. J., Dratz, E. A., and Hamm, H. E. (2001) *J. Biol. Chem. 276*, 2333−2339.
63. Arimoto, R., Kisselev, O. G., Makara, G. M., and Marshall, G. R. (2001) *Biophys. J. 81*, 3285−3293.
64. Delaglio, F., Grzesiek, S., Vuister, G., Zhu, G., Pfeifer, J., and Bax, A. (1995) *J. Biol. NMR 6*, 277−293.
65. Goddard, T. D., and Kneller, D. G. SPARKY 3, University of California, San Francisco, CA.
66. Osawa, S., and Weiss, E. R. (1995) *J. Biol. Chem. 270*, 31052−31058.
67. Garcia, P. D., Onrust, R., Bell, S. M., Sakmar, T. P., and Bourne, H. R. (1995) *EMBO J. 14*, 4460−4469.
68. Cai, K., Itoh, Y., and Khorana, H. G. (2001) *Proc. Natl. Acad. Sci. U.S.A. 98*, 4877−4882.
69. Itoh, Y., Cai, K., and Khorana, H. G. (2001) *Proc. Natl. Acad. Sci. U.S.A. 98*, 4883−4887.
70. Loewen, M. C., Klein-Seetharaman, J., Getmanova, E. V., Reeves, P. J., Schwalbe, H., and Khorana, H. G. (2001) *Proc. Natl. Acad. Sci. U.S.A. 98*, 4888−4892.

BI0268899